Threshold electronic structure at the oxygen *K* edge of 3*d*-transition-metal oxides: A configuration interaction approach

J. van Elp
Hiroshima Synchrotron Radiation Center, Hiroshima University, 2-313 Kagamiyama, Higashi-Hiroshima 739-8526, Japan

Arata Tanaka
Department of Quantum Matter, ADSM, Hiroshima University, 1-3-1 Kagamiyama, Higashi-Hiroshima 739-8526, Japan
(Received 28 December 1998; revised manuscript received 17 March 1999)

It has been generally accepted that the threshold structure observed in the oxygen *K*-edge x-ray absorption spectrum in 3*d*-transition-metal oxides represents the electronic structure of the 3*d* transition metal. There is, however, no consensus about the correct description. We present an interpretation which includes both ground-state hybridization and electron correlation. It is based on a configuration-interaction cluster calculation using an MO_6 cluster. The oxygen *K*-edge spectrum is calculated by annihilating a ligand hole in the ground state, and is compared to calculations representing inverse photoemission experiments in which a 3*d* transition-metal electron is added. Clear differences are observed related to the amount of ligand holes created in the ground state. Two ''rules'' connected to this are discussed. A comparison with experimental data of some early transition-metal compounds is made, and shows that this simple cluster approach explains the experimental features quite well. [S0163-1829(99)03028-3]

INTRODUCTION

Transition-metal oxides have attracted attention for several decades, with interest being revived in recent years because of the discovery of Cu-based high-T_c superconductors and Mn-based colossal magnetoresistance perovskites. High-energy spectroscopies like x-ray photoemission spectroscopy, Bremsstrahlung isochromat spectroscopy (BIS), and x-ray-absorption spectroscopy at the transition-metal *L* edges and oxygen *K* edges[1–4] or the energy-electron-loss spectroscopy (EELS) features at these edges[5–7] have played a key role in describing the underlying electronic structure of transition-metal oxides. Experiments at the oxygen *K* edge have determined, for instance, the amount of oxygen holes upon doping in the high-T_c superconductors,[1,2] and have recently been used to study the electronic structure of the manganese perovskites.[3]

Soft-x-ray absorption at the oxygen *K* edge is a dipole-allowed transition in which an oxygen 1*s* electron is promoted to an empty 2*p* (*np*) oxygen orbital. Although the transition involves oxygen orbitals, the threshold structure observed at the oxygen *K* edge is determined by the electronic structure of the 3*d*-transition-metal ion. The 3*d* transition metal is important because the oxygen 2*p* shell is full in an ionic picture. Empty oxygen 2*p* orbitals are created by ground-state hybridization between 3*d*-transition-metal and oxygen 2*p* orbitals. After the absorption process, the extra electron is located on the 3*d* transition-metal ion. This would suggest that oxygen *K*-edge absorption can be interpreted in a similar way as 3*d* electron addition experiments like BIS.

This approach, by which energy positions deduced at the oxygen *K* edge are used as 3*d* electron addition states, was recently used to study the electronic structure of a Mn perovskite system.[3] It is for a part based on work by de Groot *et al.*,[8] who described the threshold structure at the oxygen *K* edge as resulting from a combination of ligand field splitting and exchange coupling of the 3*d* transition metal. The intensity or spectral weight at the oxygen *K* edge is directly related to the number of unoccupied 3*d* electrons. For the less than half-filled 3*d* shell transition-metal systems, the splitting of the two threshold peaks was ascribed to ligand field splittings, but the relative intensities of the peaks could not be fully explained.

The peak positions of the empty 3*d* electron orbitals for the three most common oxidation states of Mn were obtained from molecular-orbital theory,[9] and compared by Kurata and Colliex[5] to the oxygen *K*-edge EELS. The intensities were again taken as equal to the number of unoccupied electrons in each molecular orbital.

The mechanism by which the intensity is obtained is not explained in either of these studies. Starting from an ionic approach with full 2*p* orbitals, the intensity is obtained from the ground-state hybridization between the 3*d* transition orbitals and the oxygen 2*p* orbitals. As shown in experiments by Kuiper *et al.*,[10] the strength of the hybridization is important. They compared the oxygen *K*-edge spectrum of $La_{2-x}Sr_xNiO_4$ directly with the high-energy inverse photoemission spectrum. In the inverse photoemission data, a clear empty La 4*f* structure is present at 9 eV above the Fermi level. The intensity decreases upon Sr substitution. This La 4*f* structure is virtually nonexistent in the oxygen *K*-edge spectrum, because of the absence of a significant hybridization between the oxygen 2*p* and the very localized La 4*f* core valence orbitals. This clearly establishes that the strength of the hybridization is important and must be included in the models used. Counting only the number of unoccupied 3*d* orbitals to determine the intensity is not sufficient.

Hybridization is included if one compares the oxygen *K* edge with the oxygen 2*p* projected density of states obtained

 ©1999 The American Physical Society

from band structure calculations. For the d^0 compounds $SrTiO_3$ and TiO_2, the oxygen $2p$ projected density of states showed a good agreement with the oxygen K-edge spectrum.[11] No influence of the oxygen core hole potential on the spectrum in the form of shifts of spectral weight was observed. Besides the d^0 compounds, a few oxygen K edges of $3d^n$ systems have been described using oxygen $2p$ projected density of states.[12–14] For CuO, it was found that the oxygen $2p$ orbitals are present up to 15 eV above the threshold and that the oxygen K edge shows a structure connected to $2p$, but not $3p$, levels, up to 15 eV above the threshold.[14]

What is absent in all the mentioned interpretations is electron correlation. If we accept that the threshold structure is connected to addition of $3d$ electrons, then starting from the ionic picture ($3d^n$) an electron from the oxygen band must be transferred to the $3d$-transition-metal atom to obtain oxygen $2p$ holes ($3d^{n+1}\underline{L}$, where $\underline{L}$ stands for an unoccupied $2p$ oxygen orbital). Electron correlation is important and should be explicitly included when adding a $3d$ electron to the transition metal. For inverse photoemission experiments in which the final states are mainly of d^{n+1} character, multiplet structures resulting from the electron correlation are generally accepted.

In the three systems, in which the oxygen K edges have been compared to the $2p$ projected density of states, electron-correlation effects are absent. For d^0 systems,[11] only final states with one $3d$ electron can be reached, and for CuO (Ref. 14) the final states comprise a full $3d$ orbital system (d^{10}). In both systems, the $3d$ electron-electron interactions are absent. $LiCoO_2$ is a special case because of the low-spin d^6 ground state with mainly t_{2g}^6 character. The first electron addition state[15] is a single state reached by adding an electron of e_g character, so no multiplet effects are visible in the inverse photoemission spectrum as well as at the oxygen K edge.

Configuration-interaction cluster models describing the (inverse) photoemission and x-ray-absorption spectra have been quite successful. Besides hybridization, the multiplet structure in these models is included through the use of two-electron operators. In the calculations, in which clusters are used, the transition-metal atom is mostly in the middle (MO_6 cluster). However, for an oxygen K-edge calculation one would like to have the absorbing oxygen atom in the middle surrounded by its natural environment. For a rigid octahedral transition-metal monoxide, such a large cluster would consist of the middle oxygen and six surrounding transition metals, each with additional oxygen atoms. The total cluster would be OM_6O_{18}. However, for the early transition metals a large number of empty $3d$ orbitals for every metal site is needed, and the computing problem is at present not (yet) solvable. The only clusters with an oxygen in the middle used up until now are of the Cu_2O_7 type[16] or extensions of this.[17] The total number of holes is limited with one or two holes on every Cu atom.

Connected to this problem is also the fact that for perovskite oxides or other oxide systems, the clusters need to be more complicated and can have oxygen atoms at chemically different sites, which would require the use of different clusters. We have therefore used the relatively simple MO_6 cluster with oxygen molecular orbitals of t_{2g} and e_g symmetry. The total number of orbitals is 20. The computing problem has been solved for the interesting early transition metals with more than five holes in these clusters. Several studies describing the electronic spectra of valence-band photoemission and inverse photoemission have been published, enabling us to use some of these parameters.

The oxygen K-edge absorption process in our cluster calculations is a transition from a localized oxygen $1s$ core orbital to delocalized e_g and t_{2g} symmetry oxygen $2p$ orbitals. These delocalized $2p$ orbitals are combinations of all six oxygen atoms, and the main assumption is that the spectral weight to the delocalized orbitals is the same as in a calculation with the absorbing atom in the middle. The second assumption, which is necessary, is that the interaction of the oxygen core hole with the oxygen or transition-metal valence electrons can be neglected. Support for this is obtained from the bandstructure calculations for the d^0 systems,[11] which showed that the core hole has no or very little influence on the position of the final-state energy levels. This absence of core hole valence electron interaction is quite different from the situation at the $3d$-transition-metal $2p$ edges, where a strong interaction between the $2p$ core hole and $3d$ electrons[18] is present.

A similar cluster model has been used to calculate the oxygen K-edge absorption spectrum and inverse photoemission spectrum of $LiNiO_2$.[19] The trivalent Ni ground state is low spin, so addition of spin-up and spin-down electrons is possible. The character of the ground state is mainly $d^7\underline{L}$. The configuration interaction cluster calculations describe the spectral weight difference between the threshold structure at the oxygen K edge and the first part of the inverse photoemission spectrum quite well. The present results are an extension of those calculations to $3d^1$ to $3d^7$ transition-metal systems.

CALCULATIONAL DETAILS AND PARAMETERS

The cluster used is an octahedral transition-metal symmetry MO_6 cluster, and is similar to clusters used in the analysis of late transition-metal high-energy spectroscopies.[15,19,20] It has ten $3d$ orbitals and ten oxygen molecular orbitals of t_{2g} and e_g symmetry. The nonbonding oxygen orbitals are omitted. The d-d Coulomb and exchange interactions are included using atomic multiplet theory specified in terms of Racah A, B, and C parameters. If available, the free-ion values of the Racah B and C parameters, as tabulated by Griffith,[21] are used. For the Mn^{4+} system, scaled down values (80%) of calculated Hartree-Fock values are used.[18] The d^1 system Ti^{3+} has no electron correlation. Estimated values based on Ti^{2+} were used. All the parameters are listed in Table I.

The Mott-Hubbard energy U is defined as the energy needed to remove a $3d$-transition-metal electron and add it at another d^n site and it describes the transition from $d^nd^n \rightarrow d^{n+1}d^{n-1}$. The lowest-energy level of each d^n configuration is calculated with the ionic part of the transition-metal ligand field splitting ($10Dq^i$) zero.

The charge-transfer energy Δ is defined as the energy needed for transferring an electron from the lowest level of the d^n configuration to the lowest level of the $d^{n+1}\underline{L}$ configuration. The $pp\sigma$, $pp\pi$, and $10Dq^i$ parameters are zero in this definition. The hybridization between the transition-

TABLE I. Parameters used for the calculations, all values in eV. The Racah B and C parameters for trivalent Ti are estimates as the d^1 system has no two electron interactions.

	A	B	C	Δ	$pd\sigma$	$10Dq$	$pp\sigma$-$pp\pi$
Co^{2+}	5.2	0.138	0.541	5.5	1.3	0.7	0.7
Fe^{2+}	5.5	0.131	0.483	7.0	1.3	0.7	0.7
Mn^{2+}	3.9	0.119	0.412	8.8	1.3	0.7	0.7
Fe^{3+}	4	0.126	0.595	5	1.9	1.3	0.8
Mn^{3+}	5	0.141	0.456	5	2.1	1.3	0.8
Cr^{3+}	5	0.128	0.477	5	2.3	1.3	0.8
Mn^{4+}	5	0.132	0.497	4	2.5	1.5	0.8
V^{3+}	5	0.106	0.516	5	2.3	1.3	0.8
Ti^{3+}	5	0.1*	0.5*	5	2.3	1.3	0.8

metal $3d$ states and the ligand $2p$ orbitals is taken into account by the Slater-Koster[22] $pd\sigma$ and $pd\pi$ transfer integrals. They describe the overlap between the oxygen and transition-metal orbitals for σ and π bonding. According to Harrison,[23] the value of $pd\pi$ is fixed at $pd\pi = -0.45pd\sigma$.

The Slater-Koster[22] nearest-neighbor oxygen interactions $pp\sigma$ and $pp\pi$ split the oxygen states in a double degenerate level with e_g symmetry at $pp\sigma$-$pp\pi$ and a triple degenerate level with t_{2g} symmetry at $-(pp\sigma$-$pp\pi)$. The width of the oxygen band determines the value of $pp\sigma$-$pp\pi$.

In the ground state, charge-transfer levels up to $d^{n+2}\underline{L}^2$ are included, while in the final states only one charge-transfer level ($d^{n+2}\underline{L}$) is included. In the final state, the energy difference between d^{n+1} and $d^{n+2}\underline{L}$ is $U+\Delta$, which means that double charge-transfer states are at very high energy and can be neglected.

Probably the most important parameter is the ionic $10Dq^i$ splitting. It splits the $3d$ orbitals in e_g and t_{2g} orbitals at $+6Dq$ and $-4Dq$, respectively. This splitting has not always been included in the analysis of valence-band photoemission spectra because the splittings it induces in the electron removal final states are rather small as compared to the valence-band width. For NiO and CuO, the valance-band widths are about 12 eV, and for both a good result[24,25] can be obtained without the use of an ionic $10Dq^i$. The main reason is that the overall width is obtained from hybridization between almost degenerate d^{n-1} and $d^n\underline{L}$ final states.

If the same parameters are to describe the forbidden $3d$-$3d$ optical transitions, an ionic $10Dq^i$ splitting must be added.[19] This is most apparent for the d^3 system. The experimentally determined $10Dq$ splitting between the $^4A_{2g}$ ground state and $^4T_{2g}$ excited state is about 2 eV for Cr^{3+},[26] and is independent of Racah B and C parameters. Neglecting the ionic $10Dq^i$ contribution, one finds a calculated splitting of less than 1 eV using the MO_6 cluster. The splitting is caused by a difference in transfer integrals ($pd\sigma$,$pd\pi$) for e_g and t_{2g} electrons in the hybridization between d^n and $d^{n+1}\underline{L}$ configurations. For the Cr^{3+} system, an ionic $10Dq^i$ of about 1.3 eV needs to be added to obtain the correct experimental $10Dq$ splitting of 2 eV between the $^4A_{2g}$ and $^4T_{2g}$ states.

The ionic $10Dq^i$ value was determined for the Fe^{3+} system using published optical transitions[27] of Fe^{3+} impurities in Al_2O_3. In the Cr^{3+} system, the optical $10Dq$ value is independent of Racah B and C parameters, while for the Fe^{3+} system these parameters also determine the optical splittings. For both systems an ionic $10Dq^i$ of 1.3 eV (Ref. 28) is obtained, and this value was also used for the d^1, d^2, and d^4 systems. A detailed analysis of the optical transitions in configuration-interaction cluster calculations will be presented[28] in the near future.

The value of the full $10Dq$ splitting is different for different final states and is hybridization dependent. For MnO,[29] the optical $10Dq$ is 1.2 eV with hybridization between d^5 and $d^6\underline{L}$, with an energy difference determined by the charge-transfer energy Δ. For the $^5T_{2g}$-^5E_g splitting in photoemission and inverse photoemission spectra,[20] values of 1.9 eV (d^4 and $d^5\underline{L}$, $\Delta - U$ apart) and 1.0 eV (d^6 and $d^7\underline{L}$, $\Delta + U$ apart) are obtained. The stronger the hybridization due to the proximity of the levels involved, the larger is the splitting.

The values for the trivalent Mn and Fe systems of the transfer integral $pd\sigma$ are obtained by increasing the integrals from the values of the divalent Mn and Fe systems. Values for $pd\sigma$, based on fitted tight-binding parameters to a linearized muffin-tin orbital band-structure calculation for $LaMO_3$ perovskites systems (M ranges from Ti to Ni),[30] are, for the early transition metals, around 2.3 eV. This value was chosen for trivalent Ti to Cr systems, while for the trivalent Mn (Ref. 30) system 2.1 eV was used. For the trivalent Fe system, a slightly larger value as compared to the $LaMO_3$ systems is deduced.

The optical $10Dq$ transition in Mn^{4+}-doped Al_2O_3 is around 2.4 eV.[31] Besides the larger $10Dq$ splitting, a larger covalency is also expected, so the ionic $10Dq^i$ is increased to 1.5 eV and $pd\sigma$ to 2.5 eV, whereas the charge-transfer energy Δ for Mn^{4+} systems is decreased to 4 eV.

The parameters for the Mn^{2+}, Fe^{2+}, and Co^{2+} systems are obtained from an analysis of combined photoemission and inverse photoemission experiments using similar configuration-interaction cluster calculations.[15,20,32] The obtained values for the Racah parameter A and Δ are used. The parameters obtained from an analysis of the $2p$ resonant photoemission spectra are quite similar.[33]

The inverse photoemission or BIS is calculated using the addition of a $3d$ electron. Instead of electron addition, a ligand hole of oxygen character is annihilated in the oxygen K-edge calculations. If the oxygen core hole is omitted both processes reach the same final states, d^{n+1} and $d^{n+2}\underline{L}$, but the branching ratios are different. Annihilating a ligand hole

in our cluster describes the transition at the oxygen edge as mainly a $d^{n+1}L \rightarrow \underline{c}d^{n+1}$ (where $\underline{c}$ stands for the oxygen core hole).

Formally, the intensity of the inverse photoemission experiment (BIS) $I_{\mathrm{BIS}}(E_e)$, which is a function of the incident electron energy E_e, is given by

$$I_{\mathrm{BIS}}(E_e)=\sum_{f,\tau,\sigma}|\langle f|d^{\dagger}_{\tau,\sigma}|g\rangle|^2\delta[E_f-(E_e-\hbar\omega_p)-E_g],$$

while the oxygen K-edge absorption spectrum $I_{\mathrm{O}\,1s}(\omega)$, which is a function of the incident photon energy $\hbar\omega$, is given by

$$I_{\mathrm{O}\,1s}(\omega)=\sum_{f,\nu,\sigma}|\langle f|l_{\nu,\sigma}|g\rangle|^2\delta(E_f-\hbar\omega-E_g).$$

E_g and $|g\rangle$ denote the eigenvalue and eigenfunction of the ground state, and E_f and $|f\rangle$, those of the final states. In inverse photoemission, the incoming electron is at a high-energy E_e, and the spectrum is measured by analyzing the number of photons of energy $\hbar\omega_p$ upon deceleration of the electron into a final state just above the Fermi level. The operator $d^{\dagger}_{\tau,\sigma}$ creates a $3d$ electron with spin quantum number σ at the orbital labeled τ, while the operator $l_{\nu,\sigma}$ annihilates a hole with spin quantum number σ at the ligand orbital labeled ν. The core hole and its interactions with the oxygen or transition-metal atoms are ignored in the calculations. Note that our results are identical to those obtained from a MO_6 cluster calculation with all O $2p$ orbitals included, if we neglect the O $2p$ on site Coulomb interaction.

RESULTS

The calculations are divided into two groups. In Fig. 1, the BIS and oxygen K-edge spectra of systems with five or more $3d$ electrons are shown. Here the number of final states is limited because the only electron addition possible is always a minority spin electron. For d^8 in O_h symmetry (NiO) and d^9 systems (CuO and the parent systems of the high-T_c superconductors), the number of possible final states is limited to one. From d^4 downwards, the number of final states changes, and a much larger number can be reached (see Fig. 2). Besides a minority-spin electron, now the possibility of adding a majority-spin electron also exists.

The scaling between the two calculations is such that the least effected peak in the oxygen K-edge calculation (O $1s$) has the same strength as in the BIS calculation. This is almost always the lowest-energy final state, where an e_g electron is added. For convenience, the lowest-energy final states in the figures are aligned to each other at 1 eV. It is clear that the intensity of some final states changes significantly between the two types of calculations.

The positions of the final states reached for $n \geqslant 5$ are similar to the positions in the optical spectrum of the d^{n+1} system, in which only spin-allowed transitions are observed.[34] The spin-flip transitions are not accessible. For Co^{2+}, the final states obtained are of $^3A_{2g}$, $^3T_{2g}$, $^3T_{1g}$, and $^3T_{1g}$ symmetry, and for the d^5 systems only two final states of $^5T_{2g}$ and ^5E_g symmetry are obtained. In Fe^{2+}, there are three instead of the expected four final states with $^4T_{1g}$, $^4T_{2g}$, and $^4T_{1g}$ symmetry. $^4A_{2g}$ symmetry cannot be reached with the addition of an e_g or t_{2g} electron from a $^5T_{2g}$ ground state.

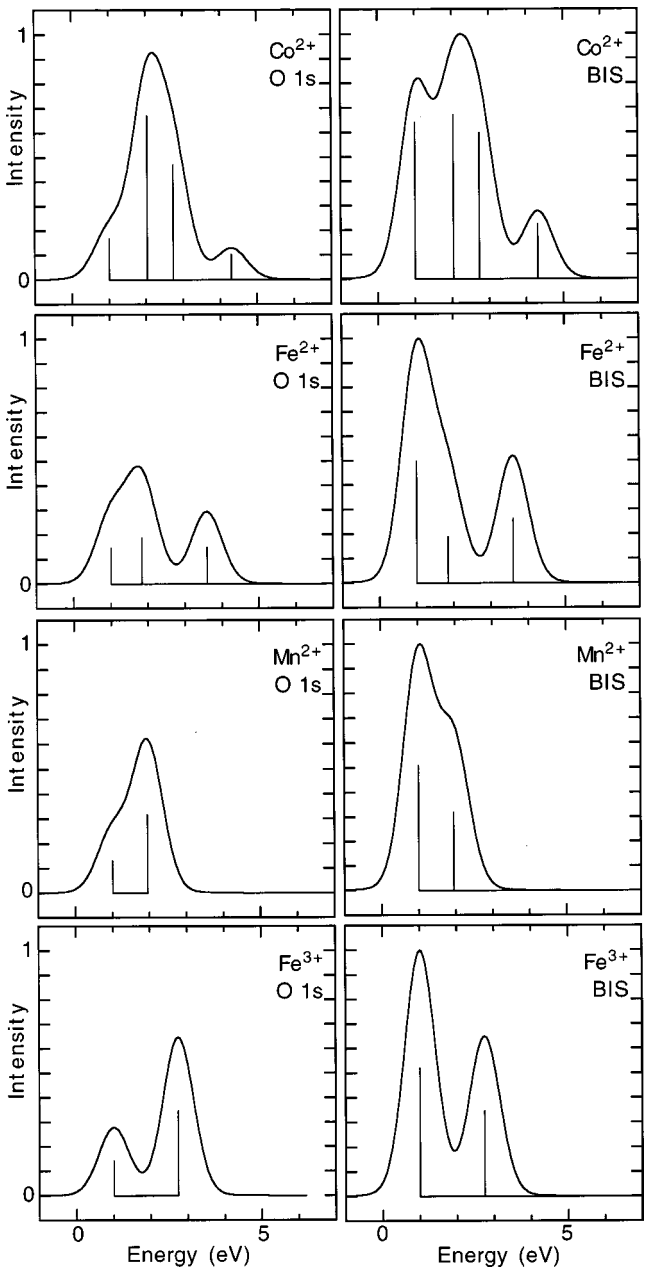

FIG. 1. Oxygen K-edge and inverse photoemission (BIS) calculations for the d^7 to d^5 systems Co^{2+}, Fe^{2+}, Mn^{2+}, and Fe^{3+}. A standard broadening of 0.8 eV is used. The sticks show the strength of individual final states.

For the $n<5$ systems, the number of final states is much larger. The lowest-energy electron addition state is the ground state for the $n+1$ system. The lowest-energy electron addition state is formed by adding an electron determined by Hund's rule. It has $^3T_{1g}$ symmetry for d^1, and $^4A_{2g}$ symmetry for d^2, both with the addition of a majority-spin t_{2g} electron in the lowest-energy final state. The ^5E_g symmetry for d^3 and $^6A_{1g}$ symmetry for d^4 are reached both with the addition of a majority spin e_g electron. The oxygen ligands in transition metal oxides are not strong enough to create low-spin ground states. The lowest-energy electron addition state is of the same character as based on ligand field and

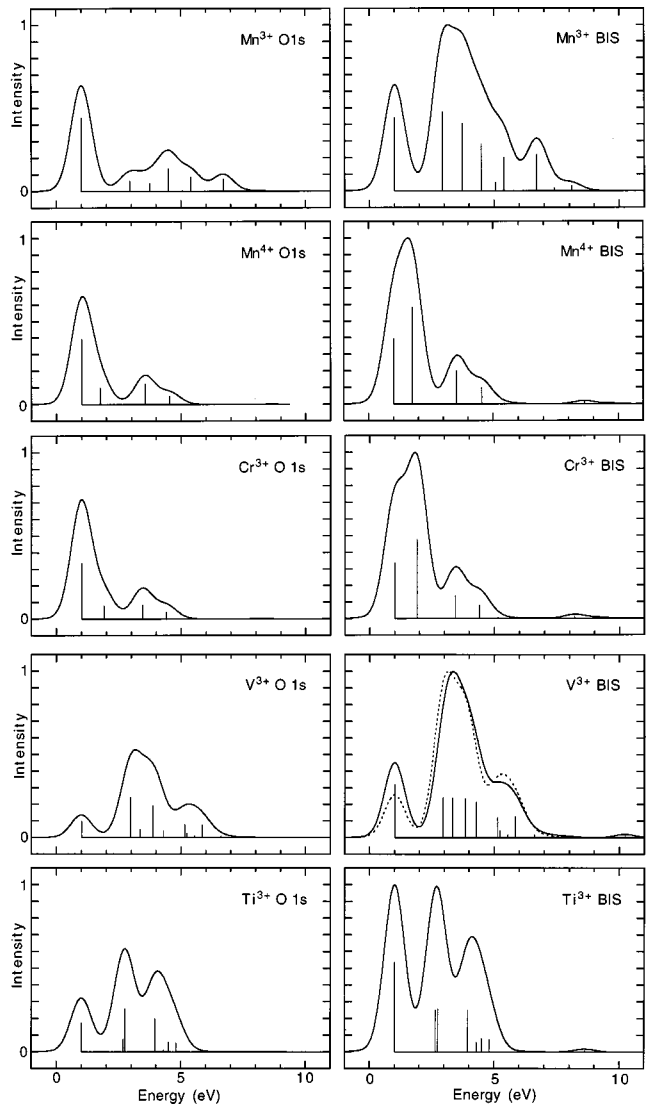

FIG. 2. Oxygen *K*-edge and inverse photoemission (BIS) calculations for d^4 to d^1 systems. A standard broadening of 0.8 eV is used. The sticks show the strength of individual final states.

exchange arguments, but is in all the calculations clearly separated from the remaining multiplet structure.

Figure 3 shows the qualitative difference between $3d$ electron addition and oxygen hole annihilation. Simplified, the electron addition process is $d^n \rightarrow d^{n+1}$. The individual strength of the final states is determined by the Wigner coefficients connected to each individual final-state transition. The annihilation of an oxygen hole can be described in a simplified picture as $d^{n+1}\underline{L} \rightarrow c\underline{d}^{n+1}$, omitting the core hole. The transition is straightforward and the strength is directly connected to the amount of ligand hole present for a certain symmetry in the ground state. By mixing the $d^{n+1}\underline{L}$ states into the ground state, the Wigner coefficients are of course involved, and determine for a part the amount of mixing possible for each $d^{n+1}\underline{L}$ state. But besides these coefficients, the amount of overlap or the size of the transfer integrals is important. To understand their influence on the oxygen *K*-edge spectrum simple perturbation theory arguments can be used.

In first order perturbation theory, the amount of $d^{n+1}\underline{L}$ mixed into the d^n ground-state wave function is equal to

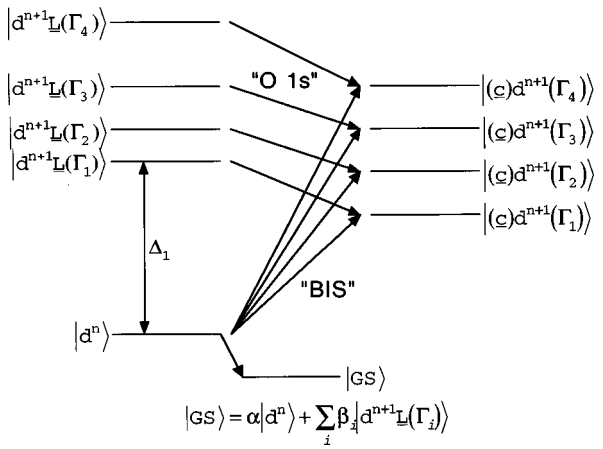

FIG. 3. Schematic picture of the difference between an oxygen *K*-edge x-ray absorption experiment and an inverse photoemission experiment (BIS). The transitions which describe in a simple picture the two transitions are labeled O 1*s* and BIS.

T/Δ, with T the transfer integral or overlap integral, and Δ the energy difference between the ground state and the perturbing level. The amount of ligand hole created in this way is equal to $(T/\Delta)^2$. From this, it is directly possible to deduce two important rules for the interpretation of the oxygen *K* edges threshold electronic structure.

First, the ligand hole created upon the transfer of an e_g electron results in an intensity in the spectrum that is four times stronger than for t_{2g} electrons, as compared to the d^n electron addition spectra. The transfer integrals for e_g electrons are about two times as strong as for t_{2g} electrons ($pd\pi = -0.45pd\sigma$), which means that the actual ligand hole amount is about four times as large.

Second, charge-transfer states, which are higher in energy, have less intensity in the oxygen *K*-edge spectrum, because the amount of ligand hole created in the ground state is smaller. This depends strongly on the charge-transfer energy Δ. If Δ is small, the differences in energy within the $d^{n+1}\underline{L}$ charge transfer states are large and the first peak is more pronounced. For large Δ, this effect will hardly be noticeable.

The effect of both rules can be seen in almost all the systems. The lowest-energy electron addition state for the d^1, d^2 and d^n, $n \geqslant 5$, are all reached by the addition of a t_{2g} electron. In all these systems, the lowest-energy electron addition state has a significantly lower intensity at the oxygen *K* edge as compared to the BIS spectrum. For the d^4 system Mn^{3+}, the lowest-energy electron addition state of $^6A_{1g}$ symmetry is the only possible way of adding an e_g majority-spin electron. The first minority-spin e_g electron addition state is at 4.5 eV and it has lost intensity as compared to the $^6A_{1g}$ state, because its charge-transfer energy Δ is much larger. For the d^3 and d^4 systems, the oxygen *K*-edge spectrum is almost fully made up of final states connected to the addition of e_g electrons. The differences between BIS and the oxygen *K* edge are large. For d^1 and d^2, the main difference is the first peak because the overall distribution of e_g and t_{2g} electron addition final states is similar. This can be seen in the V^{3+} BIS spectrum, where the oxygen *K*-edge spectrum has also been plotted (see Fig. 2) normalized to the

same maximum. Overall, the effects of both ''rules'' are clearly visible.

The energy positions at the oxygen *K* edges are not very sensitive to small changes in parameters except for the ionic $10Dq^i$ contribution. This parameter together with the Racah *B* and *C* parameters determine the mainly splittings. A change from $10Dq^i=0.7$ eV for Mn^{2+} to 1.3 eV for Fe^{3+} increases the $^5T_{2g}$ to ^5E_g splitting from 0.9 to 1.7 eV. The increase from the larger transfer integrals of Fe^{3+} is limited. The Racah *B* and *C* parameters are fixed, values chosen based on the free atom values for each individual ion. Changes in the oxygen bandwidth factorized in $pp\sigma$-$pp\pi$ do not effect the overall spectrum much. The electron removal spectrum in cluster calculations is very sensitive to the difference between *U* (through the Racah *A* parameter) and Δ. This is not the case for electron addition, where the next possible energy position for hybridization in the final states is at $U+\Delta$. Compared to the amount of d^n character in the ground states, the final states have a larger amount of d^{n+1} character.

COMPARISON WITH EXPERIMENTAL SYSTEMS

In Fig. 4, the calculated results for the oxygen *K* edge are compared with experimental spectra obtained from the literature for d^3 ($LiMnO_3$),[13] d^2 ($LiVO_2$),[35] and the d^1 systems Ti_2O_3 (Ref. 8) and $LaTiO_3$ (Ref. 36). In transition-metal systems with $n<5$, the majority-spin band is not full. In addition to minority-spin electrons, majority-spin electrons can also be added. The possible number of final states is much larger, and the width of the final state multiplet spectrum is much larger too, and therefore a more meaningful comparison with experimental systems can be made.

The features at threshold of the $LiMnO_3$ oxygen *K*-edge spectrum are well reproduced in the calculation. In the original work by de Groot *et al.*,[8] and in the molecular-orbital calculations,[5,9] the interpretation for d^3 systems is different. The first peak, which in our case is the addition of a majority-spin e_g electron, is explained as a combination of majority-spin e_g and minority-spin t_{2g} bands with relative intensities of 40% and 60%, respectively. The intensities are equal to the number of empty $3d$ orbitals. The second peak, which in our case mainly consists of minority-spin e_g electron addition, split by multiplet structure, is now only a minority-spin e_g band. Because of hybridization, the t_{2g} electron addition shows up weakly in the cluster calculations, and is positioned in between the two e_g related structures.

The electronic structure of $LiVO_2$, including the phase transition at 460 K, has been discussed extensively by Pen *et al.*[35] It is clear that the overall shape of the oxygen *K*-edge spectrum is reproduced quite well. The first peak can be identified as electron addition of a majority spin t_{2g} electron. The e_g bandwidth is large, and the t_{2g} structure is only visible as a shoulder of the e_g-derived structures at 536 eV.

In both $LiVO_2$ (Ref. 37) and the $LiMnO_3$ (Ref. 38) systems, the transition-metal ion is in a close to octahedral symmetry. In both systems, the Li plays no role in the electronic structure. This transition-metal octahedral symmetry is not observed in Ti_2O_3. The TiO_6 octahedra are distorted along the trigonal axis,[39] and three metal oxygen bond distances are 2.08 Å and three are 2.01 Å. Besides this distortion, the

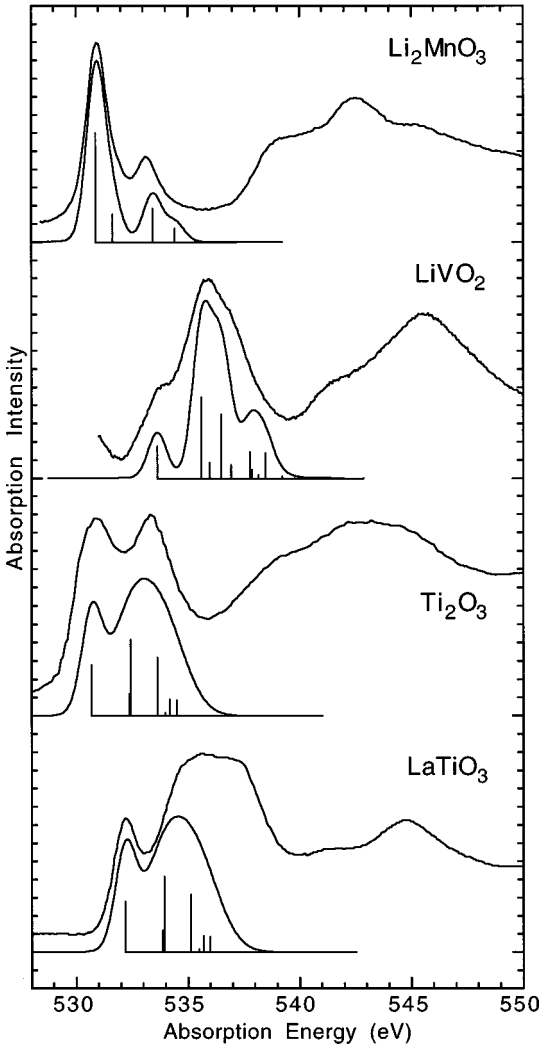

FIG. 4. Comparison between the experimental oxygen *K* edges and the calculations for the d^1, d^2, and d^3 systems $LaTiO_3$, Ti_2O_3, $LiVO_2$, and $LiMnO_3$. In the d^1 calculation the final states beyond 1 eV are broadened with 1.7 eV, because of the much larger bandwidth of e_g electrons.

Ti atoms also have one Ti neighbor with a short metal-to-metal distance, which points to possible metal-to-metal interactions as proposed by Goodenough.[40] The trigonal distortion splits the t_{2g} orbitals into an a_1 and double degenerate *e* symmetry orbital. The e_g orbitals do not split but change symmetry to *e* as well and hybridize with the *e* symmetry orbitals derived from the t_{2g} orbitals. The splitting of the t_{2g} orbitals is only important for the t_{2g}-derived first final state, which obtains extra width.

More important, however, is that the distortion, which also changes the bond angles of the octahedron, mixes the e_g ($pd\sigma$) and t_{2g} ($pd\pi$) transfer integrals. The amount of ligand hole created for e_g or t_{2g} charge transfer changes. This means that for the Ti calculation, the t_{2g}-derived first peak obtains more intensity. This effect is already visible at the oxygen *K* edge of Ti_2O_3, combined with the fact that the e_g electron addition final states have a much larger bandwidth. Overall, the width observed at the threshold is comparable to the width of the multiplet structure calculated, although the exact intensities are not fully reproduced.

The last experimental system to discuss is $LaTiO_3$. In addition to Ti, the La empty orbitals can also hybridize with oxygen orbitals, as is evident from the structure observed at 535 eV, which is not only connected to Ti but also to La empty orbitals. The first peak at the oxygen *K* edge can be identified clearly as a Ti empty orbital with majority-spin t_{2g} character only. In this system, we also have chemically different oxygen atoms, one in the LaO layer and one in the TiO_2 layer.

DISCUSSION

In the previous section, we compared our calculated results to experimental systems with a less than half-filled $3d$ shell. The d^2 and d^3 systems show quite clearly that at the oxygen *K* edge we observe an electronic structure described by a combination of electron correlation, ionic contribution to ligand field splitting, and, most importantly, by hybridization between the oxygen and transition-metal atoms in the ground state. The actual amount of ligand holes created in the ground state is instrumental for a correct understanding of the experimental features at the oxygen *K* edges.

In systems more than half-filled, such a clear cut situation is not observed. The different interpretations cause differences in the strength of the final states and in energy positions between our approach and results based on ligand field splittings[8] or oxygen $2p$ partial density of states obtained from band-structure calculations. The widths of the calculated oxygen *K*-edge spectra and of the calculated BIS spectra are more or less similar for all the different interpretations, and a limited number of features is observed in the experimental spectra.[15] Overall, it is difficult to judge and give full credit to a certain interpretation for d^n, $n \geqslant 5$, systems.

The expected strength connected to the e_g electrons final states is not always experimentally observed. In $LaFeO_3$,[41] the second peak connected to the addition of an e_g electron has only slightly more intensity than the first peak connected to a t_{2g} orbital. Both e_g electrons point toward their oxygen neighbors, and because of this they have a much larger bandwidth. This means that if the e_g bandwidth is much larger than the corresponding t_{2g} bandwidth, the relative intensity of the e_g peaks will go down, and also that e_g peaks can overlap the t_{2g} peaks. This overlap is likely present in MnO (Ref. 8) and CoO,[15] as no clear t_{2g} structure is visible in these two systems. In both oxygen *K*-edge spectra, the rise at threshold is much slower than that which should be expected based on the resolution used. The same situation is observed for the $LiVO_2$ system. Here the first structure connected to t_{2g} orbitals is only present as a shoulder on the wide e_g-related structure.

The first-order perturbation theory approach shows the extent of the influence of the hybridization on the strength of the oxygen *K*-edge spectrum as compared to the inverse photoemission spectrum. It is important to realize that both ''rules'' are independent of the chosen cluster approach. They are quite similar for a single oxygen ion interacting with a transition-metal ion, because they are obtained from a simple perturbation approach. The fact that the calculations work so well for the $LiVO_2$ and $LiMnO_3$ systems is due to the two simple ''rules.''

The oxygen *K* edge is sensitive to changes in local transition-metal geometry because of the strong dependence on hybridization. A small distortion, which in the BIS spectrum will split a peak with a few hundred meV, and which has little influence on the overall spectrum due to a large bandwidth, has a large effect on the oxygen *K* edge. The size of the transfer integrals changes because the σ and π overlap changes. An angle distortion mixes them, and this mixing changes the intensity to a much greater extent than that which would be observed in the corresponding BIS spectrum. The oxygen *K*-edge intensity is also not normalized to the amount of empty $3d$ orbitals as a BIS experiment is for most systems.

As compared to our calculation, the local Ti geometry in Ti_2O_3 will increase the intensity of the first features of t_{2g} character in the oxygen *K*-edge spectrum. The overall width is obtained but the intensities are not fully reproduced. The $LaTiO_3$ spectrum also shows the difficulty in understanding the oxygen threshold structure, because both metals are hybridizing with oxygen atoms. The first peak can be identified as a majority-spin t_{2g} orbital or band.

The local geometry also plays a major role in the Jahn-Teller d^4 systems. The two atoms on the *z* axis have an elongated or shortened distance to the transition-metal ion. The degeneracy of the e_g electrons is lifted, and, depending on the distortion, the occupied orbital is the $d_{x^2-y^2}$ (shortened) or the d_{z^2} (elongated). Two chemically different oxygen atoms are created. The lowering of the symmetry leads to extra ligand field parameters,[34] *Ds* and *Dt*, which describe the splitting between the two e_g electrons and between the t_{2g} electrons. We have not attempted to compare our calculations with a d^4 system, mainly for the following reasons.

The hybridization with the *z* axis oxygen atoms changes with the distortion. Depending on the out-of-plane to in-plane bond distance, this can be described with transfer integrals connected to the *z* axis and to the in-plane *xy* direction. The overlap integral[23] changes with the distance ratio to the power 3.5. For a 15% elongation, this change is 63%, which means T^2 is about a factor of 2.6 larger. For an elongated system, the strongest hybridized orbital would then be the $d_{x^2-y^2}$. This would be the first e_g-derived final state in our calculations, reached upon filling the majority spin $d_{x^2-y^2}$. The strongest intensity minority-spin orbital would also be the $d_{x^2-y^2}$. The position of the energy level of these orbitals would be the main problem, because one can also expect an ionic contribution to the splitting of the e_g orbital and the splitting of the t_{2g} orbital. The splitting between the two e_g orbitals and between the t_{2g} orbitals can be quite large. In CrF_2, a splitting of 3.1 eV between the two split e_g electrons is observed,[42] but this system also has a large bond distance ratio of 1.22. For trivalent Mn systems, values for the two split e_g orbitals of about 1 eV have been observed.[43] This splitting is not only caused by differences in hybridization, an ionic contribution is also needed. But it is not clear how large this ionic contribution to the splitting between the e_g (t_{2g}) orbitals is. Such large distortion needs a different cluster setup, where the hybridization with in-plane and out-of-plane oxygen atoms is properly taken into account.

The last point to mention is possible $3d$-transition-metal threshold structures for other ligands than oxygen. One would expect to see the same spectral features at the fluoride

K edge (~790 eV), although with a significantly smaller intensity because of a much smaller ground-state hybridization between the fluoride $2p$ orbital and transition-metal $3d$ orbital.

CONCLUSIONS

The threshold structure observed in the oxygen *K*-edge x-ray-absorption spectrum is determined by the electronic structure of the $3d$ transition-metal orbitals in $3d$ transition-metal oxides. The interpretation presented by us includes both ground-state hybridization with differences between σ and π bonds, and electron correlation. It is based on a configuration-interaction cluster calculation using a MO_6 cluster. The O *K*-edge spectrum is calculated by annihilating a ligand hole in the ground state, and is compared to electron addition calculations representing inverse photoemission experiments. Clear differences are observed related to the amount of ligand hole created in the ground state.

Based on the difference and using simple perturbation theory arguments, two ''rules'' can be formulated. First, the ligand holes created with the charge transfer of an e_g electron have four times more intensity than ligand holes created with charge transfer of a t_{2g} electron. The difference is directly connected to the difference in overlap integrals ($pd\sigma$ and $pd\pi$), which reflects the difference between σ and π bonding. Second, the higher the energy of a particular charge-transfer level Δ in the ground state, the weaker the intensity of this level in the oxygen *K*-edge spectrum. Both rules can explain the differences between the presented oxygen *K*-edge calculations and the electron addition calculations representing inverse photoemission spectra.

The comparison of d^2 and d^3 calculations with the oxygen *K*-edge data of $LiVO_2$ and $LiMnO_3$ shows that the oxygen *K*-edge spectral weight is described quite well by taking into account the amount of ligand holes in the ground state and the electron correlation of the $3d$ electrons. For systems with a less than half-filled shell, electron addition produces the largest energy spread in the final states because of the possibility of majority and minority spin electron addition. For d^3 and d^4 systems, the oxygen *K*-edge spectral weight is almost completely made up of e_g electron addition final states.

The comparison with the two d^1 systems Ti_2O_3 and $LaTiO_3$ also shows the limitations of our approach. Distortions of octahedral symmetry are expected to have a large influence on the oxygen *K*-edge spectrum. Mixing of the transfer integrals occurs because of mixing of σ and π bonding between the transition-metal atom and the oxygen atom. In $LaTiO_3$, the hybridization of oxygen orbitals with empty La orbitals is possible, and leads to structure at the oxygen *K*-edge overlapping the $3d$-transition-metal threshold structures.

The change of transfer integrals with distortions can have a strong effect on *z*-axis elongated d^4 Jahn-Teller systems. With a large distortion, the oxygen *K*-edge spectrum is mainly determined by final states connected to the $d_{x^2-y^2}$ orbital. The other orbitals have much smaller spectral weights. Also, such a system has two nonequivalent oxygen positions, which means that in calculations larger clusters are needed.

ACKNOWLEDGMENTS

We thank H. Pen for sending the $LiVO_2$ spectrum in digital form to us and T. Jo for a critical reading of the manuscript. This work was partly supported by a Grant-in-Aid for scientific research from the Ministry of Education, Science, Sports and Culture of Japan.

[1] C. T. Chen *et al.*, Phys. Rev. Lett. **66**, 104 (1991).
[2] C. T. Chen, L. H. Tjeng, J. Kwo, H. L. Kao, P. Rudolf, F. Sette, and R. M. Fleming, Phys. Rev. Lett. **68**, 2543 (1992).
[3] J.-H. Park, C. T. Chen, S.-W. Cheong, W. Bao, G. Meigs, V. Chakarian, and Y. U. Idzerda, Phys. Rev. Lett. **76**, 4215 (1996).
[4] S. Nakai, T. Mitsuishi, H. Sugawara, H. Maezawa, T. Matsukawa, S. Mitani, K. Yamasaki, and T. Fujikawa, Phys. Rev. B **36**, 9241 (1987).
[5] H. Kurata and C. Colliex, Phys. Rev. B **48**, 2102 (1993).
[6] H. Kurata, E. Lefêvre, C. Colliex, and R. Brydson, Phys. Rev. B **47**, 13 763 (1993).
[7] Within the small-scattering-angle approximation the x-ray absorption and high-energy electron-loss cross sections are the same; see L. A. Grunes, R. D. Leapman, C. N. Wilker, R. Hoffmann, and A. B. Kunz, Phys. Rev. B **25**, 7157 (1982).
[8] F. M. F. de Groot, M. Grioni, J. C. Fuggle, J. Ghijsen, G. A. Sawatzky, and H. Petersen, Phys. Rev. B **40**, 5715 (1989).
[9] D. M. Sherman, Am. Mineral. **69**, 788 (1984).
[10] P. Kuiper, J. van Elp, G. A. Sawatzky, A. Fujimori, S. Hosoya, and D. M. de Leeuw, Phys. Rev. B **44**, 4570 (1991).
[11] F. M. F. de Groot, J. Faber, J. J. M. Michiels, M. T. Czyzyk, M. Abbate, and J. C. Fuggle, Phys. Rev. B **48**, 2074 (1993).
[12] M. T. Czyzyk, R. Potze, and G. A. Sawatzky, Phys. Rev. B **46**, 3729 (1992).
[13] F. M. F. de Groot, Ph.D. Thesis, University of Nijmegen, The Netherlands, 1991.
[14] M. Grioni, M. T. Czyzyk, F. M. F. de Groot, J. C. Fuggle, and B. E. Watts, Phys. Rev. B **39**, 4886 (1989).
[15] J. van Elp, J. L. Wieland, H. Eskes, P. Kuiper, G. A. Sawatzky, F. M. F. de Groot, and T. S. Turner, Phys. Rev. B **44**, 6090 (1991).
[16] H. Eskes and G. A. Sawatzky, Phys. Rev. B **43**, 119 (1991).
[17] A. Tanaka and T. Jo, J. Phys. Soc. Jpn. **65**, 912 (1996).
[18] G. van der Laan and I. W. Kirkwood, J. Phys.: Condens. Matter **4**, 4189 (1992).
[19] J. van Elp, H. Eskes, P. Kuiper, and G. A. Sawatzky, Phys. Rev. B **45**, 1612 (1992).
[20] J. van Elp, R. H. Potze, H. Eskes, R. Berger, and G. A. Sawatzky, Phys. Rev. B **44**, 1530 (1991).
[21] J. S. Griffith, *The Theory of Transition Metal Ions* (Cambridge University Press, Cambridge, 1961).
[22] J. C. Slater and G. F. Koster, Phys. Rev. **94**, 1498 (1954).
[23] W. A. Harrison, *Electronic Structure and the Properties of Solids* (Freeman, San Francisco, 1980).
[24] A. Fujimori and F. Minami, Phys. Rev. B **30**, 957 (1984).

[25] H. Eskes, L. H. Tjeng, and G. A. Sawatzky, Phys. Rev. B **41**, 288 (1990).
[26] D. S. McClure, J. Chem. Phys. **38**, 2289 (1963).
[27] D. S. McClure, J. Chem. Phys. **36**, 2757 (1962).
[28] J. van Elp and A. Tanaka (unpublished).
[29] D. R. Huffman, R. L. Wild, and M. Shinmei, J. Chem. Phys. **50**, 4092 (1969).
[30] P. Mahadevan, N. Shanthi, and D. D. Sarma, Phys. Rev. B **54**, 11 199 (1996).
[31] S. Geschwind, P. Kisliuk, M. P. Klein, J. P. Remeika, and D. L. Wood, Phys. Rev. **126**, 1684 (1962).
[32] J. van Elp, Ph.D. Thesis, University of Groningen, The Netherlands, 1991.
[33] A. Tanaka and T. Jo, J. Phys. Soc. Jpn. **63**, 2788 (1994).
[34] C. J. Ballhausen, *Introduction to Ligand Field Theory* (McGraw-Hill, New York, 1962).
[35] H. F. Pen, L. H. Tjeng, E. Pellegrin, F. M. F. de Groot, G. A. Sawatzky, M. A. van Veenendaal, and C. T. Chen, Phys. Rev. B **55**, 15 500 (1997).
[36] A. Fujimori *et al.*, Phys. Rev. B **46**, 9841 (1992).
[37] W. Rudorff and H. Becker, Z. Naturforsch. B **9**, 613 (1954).
[38] P. Strobel and B. Lambert-Andron, J. Solid State Chem. **75**, 90 (1988).
[39] R. E. Newnham and Y. M. de Haan, Z. Kristallogr. **117**, 235 (1962).
[40] J. B. Goodenough, Phys. Rev. **117**, 1442 (1960).
[41] M. Abbate, F. M. F. de Groot, J. C. Fuggle, A. Fujimori, O. Strebel, F. Lopez, M. Domke, G. Kaindl, G. A. Sawatzky, M. Takano, Y. Takeda, H. Eisaki and S. Uchida, Phys. Rev. B **46**, 4511 (1992).
[42] C. Theil, J. van Elp, and F. Folkmann, Phys. Rev. B **59**, 7931 (1999).
[43] A. B. P. Lever, *Inorganic Electronic Spectroscopy* (Elsevier, Amsterdam 1984).